Carpathian Journal of Earth and Environmental Sciences, November 2012, Vol. 7, No. 4, p. 173 - 180

IDENTIFICATION OF INLAND EXCESS WATER FLOODINGS USING AN ARTIFICIAL NEURAL NETWORK

Boudewijn VAN LEEUWEN, Gábor MEZŐSI, Zalán TOBAK, József SZATMÁRI & Károly BARTA

Department of Physical Geography and Geoinformatics, University of Szeged, POB 653 Szeged, H-6701,Hungary
leeuwen@geo.u-szeged.hu, mezosi@geo.u-szeged.hu, tobak@geo.u-szeged.hu, szatmari@geo.u-szeged.hu, barta@geo.u-szeged.hu

Abstract: Inland excess water is a partly natural and partly human induced phenomenon where areas are flooded with water that cannot find its way gravitationally to rivers or channels. These inundations cause large financial and environmental damage in the flat regions of the Carpathian basin. To understand where and why the inundations occur can help to take preventive measures and to reduce loses. Inland excess water is caused by a complex and interrelated set of factors. To study these factors, a new approach using a combination of an artificial neural network (ANN) and a geographic information system (GIS) has been developed. This article presents and evaluates the results of this approach. The network is integrated in a workflow that starts and ends using multiple spatial data sets in a GIS. The intermediate steps – the training and simulation of the ANN – are performed using a mathematically modeling environment which is controlled from within the GIS. This framework allows for the flexible use of different spatial data sets and experimentation with the settings of the neural network. The training validation shows that the relief is the most important factor in the study area, while other factors like distances to anthropogenic objects are of less importance. The simulation results show that the ANN – GIS framework is capable of accurately identifying inland excess water floodings.

Keywords: Inland excess water, artificial neural networks, GIS

1. INTRODUCTION

Due to its geographic position and climate, the Great Hungarian Plain is under continuous treat of droughts and floods. The year 2010 was one of the wettest years ever in Hungary. In the period October 2009 – December 2010, 1149 mm of precipitation fell, which corresponds to a yearly precipitation of 919 mm, while the long term average yearly precipitation is 489 mm (Vízügy 2011). The extreme precipitation caused exceptionally large areas to be flooded by inland excess water. The maximum total flooded area was 355 000 ha on December 9, 2010 and the estimated financial damage to the agriculture exceeded 500 million Euros. Together with the consequential damage like soil degradation, inland excess water is one of the most severe natural hazards in the Carpathian basin (Ianos et al., 2009; Mezösi, 2011). To be able to prevent and remediate the inland excess water inundations and to understand why and where they occur, it is necessary to create accurate maps. Many, mainly Hungarian authors have presented methods to identify and/or forecast inland excess water with varying success (Bozán et al., 2009; Pálfai, 2004; Pásztor et al., 2006; Rakonczai et al., 2003). Most studies have tried to identify factors that cause inland excess water and combined them using regression functions or other linear statistical analysis. Disadvantages of these methods are that they presume that the input factors are normally distributed and that their importance has to be estimated based on expert knowledge or regression analysis which are only locally valid. A new approach using a combination of an artificial neural network (ANN) and a geographic information system (GIS) (Van Leeuwen et al., 2010) does not have these problems. This article will present and evaluate the results of this approach.

ANNs have been proven themselves in many fields of science where complex data sets need to be analyzed to identify their underlying structures and

properties. Neural networks have a large potential for analysis of complex spatial problems which are common in geographic research (Hewitson & Crane, 1994). The inland excess water inundations in the Carpathian basin are a prototype example of such a problem.

A GIS is a computational system that combines a spatial database with a set of tools for spatial analyses. It offers flexible tools to create georeferenced maps and to analyze spatial distributions within and between them.

2. INLAND EXCESS WATER IDENTIFICATION

Inland excess water is a phenomenon that is the result of a complex set of natural and anthropogenic factors. When water originating from precipitation or snow melting can neither infiltrate in the soil, nor find its way gravitationally to rivers or channels, it remains on the surface. This type of inland excess water is referred to as accumulation inland excess water. The process causes large areas to become covered with a shallow layer of water. This usually takes place after the winter period due to snow melting and rainfall, but occasionally also occurs in summer or autumn. The floodings can have large economic, social and environmental effects. The second type of inland excess water is the upwelling type and is caused by the upwards push of groundwater. The vertical type occurs as groundwater flows from higher towards lower areas, where it appears on the surface by leakage through porous soils. This normally occurs at the edges of alluvial fans. The factors causing inland excess water are divers and interrelated. The most important factors are:

(1) Relief. On the flat lands of the Carpathian basin, runoff possibilities are limited. Local depressions can collect water from a large area, without having the possibility to drain into rivers or channels.

(2) Soil. Clayey soils have a low infiltration capacity due to their chemical or physical composition or due to intensive tillage (plow pan) (Kuti et al., 2006; Rakonczai et al., 2011).

(3) Meteorology. Due to intensive rainfall or rainfall over a long period, large amounts of water need to infiltrate in the soil. Low temperatures result in low evaporation rates. Frozen soil completely prevents the infiltration of water.

(4) Anthropological factors. Human influence on inland excess water is large. On one hand, build up areas may reduce the infiltration capacity of the soil, and structures like highways may block natural runoff. On the other hand, channels and other hydrological structures reduce the change of inland excess water.

There are two methods to estimate the spatial and temporal distribution of inland excess water. The first method calculates the spatial and temporal distribution based on field or remotely sensed observations (*in situ* mapping). The second estimates the vulnerability to inland excess water based on a limited set of factors (vulnerability mapping). Systematic mapping of inland excess water has been executed since the 1940s. In earlier days, this could only be done by *in situ* observation of the inundations and drawing them on 1:10 000 and 1: 25 000 topographic base maps. *In situ* inland excess water maps have been created systematically by the regional water directorates in Hungary. This type of observations is time consuming and error prone due to differences in observation methods and quality. An inland excess water patch does not have a clear boundary, because the soil surrounding it is normally saturated with water. Due to its swampy nature, it is very difficult to measure every inland excess water patch individually in the field.

With the appearance of publically available remote sensing data, like aerial and spaceborne imagery and the development of image processing techniques, the *in situ* observations were complemented and inland excess water could be identified and classified in a more efficient and effective way (Rakonczai et al., 2003). A disadvantage of most remote sensing acquisition techniques is that they are dependent on good weather, and inland excess water is often occurring during periods with lots of precipitation. Also the dynamic nature of the floodings causes problems. Especially spaceborne remote sensors have a limited revisiting time, which may result in inaccurate measurements of inland excess water because the flooded area may have reduced in size or disappeared already by the time the satellite passed over the area. The vegetation cover may further reduce the usability of remote sensing data.

Vulnerability mapping of inland excess water is traditionally executed by selecting a limited set of factors causing the floodings and by weighing those using coefficients that are derived experimentally. The weights of the coefficients are adapted to match earlier observations or are based on expert knowledge. The weights are different for every geographical area and therefore need to be re-estimated for every region. Many authors have calculated inland excess water vulnerability maps based on such a limited set of factors like relief, soil, groundwater, precipitation etcetera (Bozán et al., 2009; Pálfai, 2003; Pásztor et al., 2006).

3. ARTIFICIAL NEURAL NETWORKS

Artificial neural networks are computational models that are mimicking the functioning of the human

brain (Hewitson & Crane, 1994). They are computational mechanisms that are able to acquire, represent, and compute a mapping from one multivariate space of information to another, given a set of data representing that mapping (Atkinson & Tatnall, 1997). In this study, a two layer feed forward network with back propagation training was applied. This is one of the most commonly used neural networks for classification problems (Demuth et al., 2010; Pradhan & Lee, 2010). In the network, every neuron processes the weighted sum of all inputs, and – via a so-called nonlinear activation function – it is determined if the signal is send further to a next layer of neurons. During the first phase of neural network modeling, input data and associated output data are fed to the network. An iterative process then adapts the weights in order to find their optimal values. The optimal values are reached when the total error between the calculated and the expected results is minimal. This is the *trained* status of the network (Hagen et al., 1996).

During the second phase of the ANN modeling, new input data is fed to the trained model and output results are generated. The quality of the result of this simulation is directly dependent on the quality of the training. If the training data set does not cover the same variation of input combinations as the simulation data set, poor output results may occur. Similarly, if the training has occurred in such a way, that the trained network can only generate results if the training input and the simulation input are the same or very similar, *over training* has occurred. This leads to poor results when a new simulation data set is fed to the network.

The artificial neural network approach has many advantages compared to other statistical methods. First, it is independent on the statistical distribution of the data, and there is no need for specific statistical variables. Neural networks allow the target classes to be defined in relation to their distribution in the corresponding domain of each data source, and therefore the integration of remote sensing and GIS data is very convenient (Pradhan & Lee, 2010). Furthermore, ANNs are capable of incorporating uncertainty, incomplete data, incorrect sampling, multicollinearity between variables, spatial or temporal autocorrelation, or the insignificance of single variables (Bishop, 1995; Yang & Rosenbaum, 2001; Zhou, 1999), which are all common in geographic analysis, but especially in inland excess water research due to the fuzzy nature of the boundaries of the inundations, and the complex interrelations between the factors that cause inland excess water.

4. DATA AND METHODS

To develop and test the ANN – GIS approach, data from a 20 km^2 large test area was collected and processed. The area is located in the south of the Great Hungarian Plain (Fig. 1) between the Tisza and Maros rivers. The relative relief energy is low, approximately 1.86 m/km^2 including artificial structures like dikes and roads.

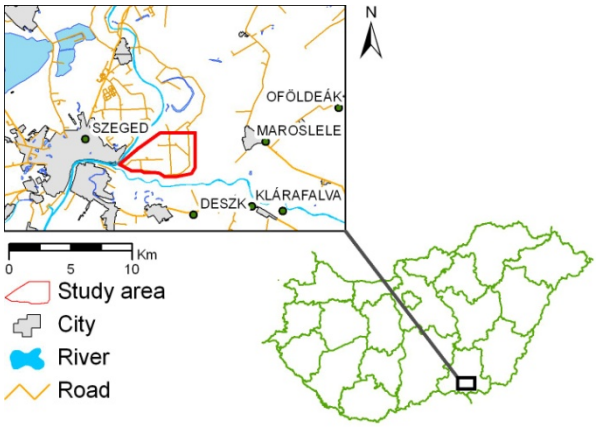

Figure 1. The study area and its surroundings.

Table 1. Base data for the ANN – GIS approach.

Light Detection And Ranging (LIDAR) DEM	LIDAR data with a spatial resolution of 1.4 points per m^2 were collected from a 70 km^2 area during a flight campaign in November 2009. Based on this data, a digital elevation model was created.
Color infra-red digital aerial photographs	At the maximum of the inland excess water periods, in March and June 2010, flights were executed using a data collection system based on a MS3100 digital camera to collect 860 x 640 meter images. From all individual images a mosaic covering an area of 60 km^2 was created.
Soil map	The 1:100 000 Agrotopo soil map was digitized and converted to raster format.
Anthropogenic objects	Channels, roads, buildings and oil wells were digitized based on the 1:10 000 topographic map, the LIDAR based digital elevation model and color aerial photographs.
Field measure-ments	In March 2010, a fieldwork was carried out in the south-western part of the study area. At that moment, the second level on the national inland excess water hazard scale was valid in the area.

Mainly agricultural activity is taking place in the area, but there are also many oil stations from the Hungarian oil company. The soils in the area show extreme mechanical properties: in large areas, the

plasticity index according to Arany (K_A) is above 60. The exceptionally bad permeability characteristics combined with the very flat terrain with large local depressions result in high vulnerability to inland excess water accumulation.

Five different base data sources were compiled and preprocesses in the GIS and transformed to input data (Table 1).

From the five data sets, 9 input layers and 1 output layer were derived and used in the framework:

(1) LIDAR measurements: At the start of the winter, while vegetation activity was minimal, but without the land being covered with snow, a combined LIDAR – digital aerial photography flight campaign was executed. At the same time of the LIDAR measurements, visual and near infrared digital images were acquired with a DMC camera. In the post-processing phase, 3D vectors of linear features were digitized from the images using stereo-photogrammical techniques and these were then incorporated in the interpolation of the LIDAR data. In this way, a digital elevation model (DEM) with a spatial resolution of 1 meter and a vertical accuracy of 15 centimeter was created (Szatmári et al., 2011). Based on this high resolution DEM, the drainage pattern was derived and local depressions were calculated. The depression map was reclassified into three depth classes: very small (<15 cm), medium (15-60 cm) and deep depressions (>60 cm). These classes are based on the accuracy of the digital elevation model and observations of inland excess water in the field. In the very flat terrain of the study area, areas that are more than 60 cm lower than the direct surroundings are ditches, channels and rivers. These should not be considered inland excess water. The areas with depressions less than 15 centimeters deep are part of the uncertainty of the elevation model. They may also be real, but then they are normally smaller puddles from where water can evaporate in a short period of time. The areas with depression between 15 and 60 centimeter deep are considered to be areas were inland excess water formation can occur.

(2) Color infrared digital aerial imagery: During different periods of large inland excess water inundations, flight campaigns were organized to collect data using an in-house developed system for small format aerial photography (van Leeuwen et al., 2009a; van Leeuwen et al., 2009b; Tobak et al., 2008). Images were collected with a spatial resolution of 62 centimeter from a flying height of 2000 meter and from the green, red and near infrared part of the electromagnetic spectrum. The three bands were used as single separate layers in the framework.

(3) The Agrotopo soil map (Agrotopo, 2002) was digitized and converted to raster format. Variations in the soil types are very limited. All three soil classes in the study area are characterized by poor permeability and a low infiltration rate.

(4) Anthropogenic objects: Based on different sources – objects built by humans that could influence the formation of inland excess water – were digitized. From these layers four distance maps were created, storing the distances between every pixel and the closest anthropogenic object.

(5) Fieldwork: During the spring inland excess water period of 2010, *in situ* measurements were taken from the inundated fields by walking around them with hand-held GPS receivers and collecting their perimeter. In total 7.8 ha of inundated land was measured with an accuracy of 2 – 5 meter.

To facilitate the efficient application of classification of inland excess water occurrences by artificial neural networks, an integrated GIS – ANN framework was created using a combination of the ArcGIS geographic information system, Matlab mathematical modeling software and Python, an open source programming language (van Leeuwen et al., 2010, Fig. 2). ArcGIS was chosen because it has strong geoprocessing capabilities. It also can be used to call external Python scripts, that are needed to connect the GIS to the ANN. Matlab was selected because of its extended Neural Network toolbox (Demuth et al., 2010) and because it can handle very large data sets. It is also possible to call and run Matlab in the background using Python scripts.

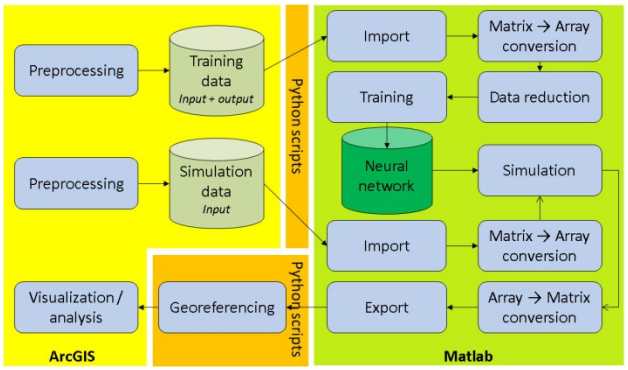

Figure 2. The framework showing the traing and simulation workflow from ArcGIS via Python to Matlab, and back.

The analysis of inland excess water with the framework is executed in several sequential steps (Fig. 2). First, the input data is pre-processed using the GIS. Here, general geoprocessing tasks are executed to generate data of the correct spatial

extent, with proper coordinates. Subsequently, using a custom made dialog in the GIS, the neural network is initiated in Matlab. Then, after conversions and data reduction, the network is trained using a training data set which is a subset of the complete data set, and a target data set. Once the network has reached its optimal state, it is saved and a message is send to the GIS that the network is ready for the simulation phase. In the simulation phase, new data is fed into the trained network using a dialog within the GIS. The simulation result is converted and georeferenced so it can be read into the GIS. Finally, the simulation results can be used for visualization and further analysis within the GIS.

Performance problems occur due to the nature of spatial data sets and the neural network method. Spatial data sets are multiple grids of large numbers of rows and columns. During the inland excess water simulations, very high resolution data is used, resulting in large amounts of data. Furthermore, the iterative process to train the network to find the optimum value for the weights for each neuron is calculation intensive. To reduce the performance problems, a data reduction factor was introduced. With this factor, only a selection of the total amount of data is used as input data. An additional advantage of the data reduction factor is that over-training of the network – when the network becomes too specialized to find general patterns in the data – is prevented.

4. RESULTS

Many experiments were executed to determine the best settings for the neural network, to evaluate the contribution of the individual layers to the solution and to estimate the overall success of the method. Earlier test with small data sets with just 4 input layers and simpler neural networks showed that the framework can be applied to calculate inland excess inundations (van Leeuwen et al., 2010). Additional data layers and more complex networks improved the classification results. Here, the most relevant results are presented.

A feed forward network with 20 hidden neurons that was trained with 8 input layers of an area of about 1000 x 1000 meter gave the best overall results. The weights of the network were randomly initialized, resulting in slight changes in the starting conditions of each training. The initialization that resulted in the best training mean square error was selected to be used in the simulation phase. The trained neural network was used for simulation in a new area slightly to the north of the training area. This way the factors that are responsible for the formations of inland excess water play a similar role in both the training and simulation. Figure 3 shows the results of the training and simulation.

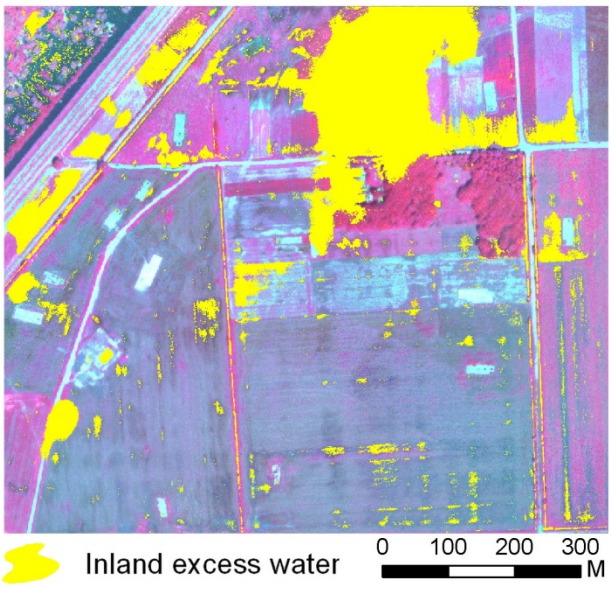

Figure 3. The simulation result for a network with 20 neurons in the hidden layer and 8 input layers.

The yellow areas were classified as inland excess water. The network was trained with the follwoing 8 input layers: the three bands of the aerial photograph, the classified local depressions map and the four distance to anthropogenic object maps. This resulted in a 93% accuracy of the training.. Figure 3 shows that in the north and northwest part of the simulation area the results are corresponding with the ground truth. The open water along the levee (in the northwest) was also detected. The large inland excess water area (in the north-northeast) was smaller in reality. The inland excess water in the south part of the images is not properly classified. Some pixels are correctly indicated as inland excess water but the majority is classified as dry land. The errors are probably due to the composition of the training set, where only water was incorporated but saturated soil and vegetation in water were omitted.

Four experiments were executed to evaluate the influence of the different input layers. Each experiment was executed with a different set of input layers, but with the same neural network consisting of 20 hidden neurons. To reduce the amount of data and to prevent running out of memory, the data reduction factor was set to 2 and Matlab's internal memory reduction factor (Demuth et al., 2010) was set to 3 in each simulation. The input layers are given in table 2. These simulations have been performed on data from the training area only, since only there, it is possible to compare the results with ground truth data.

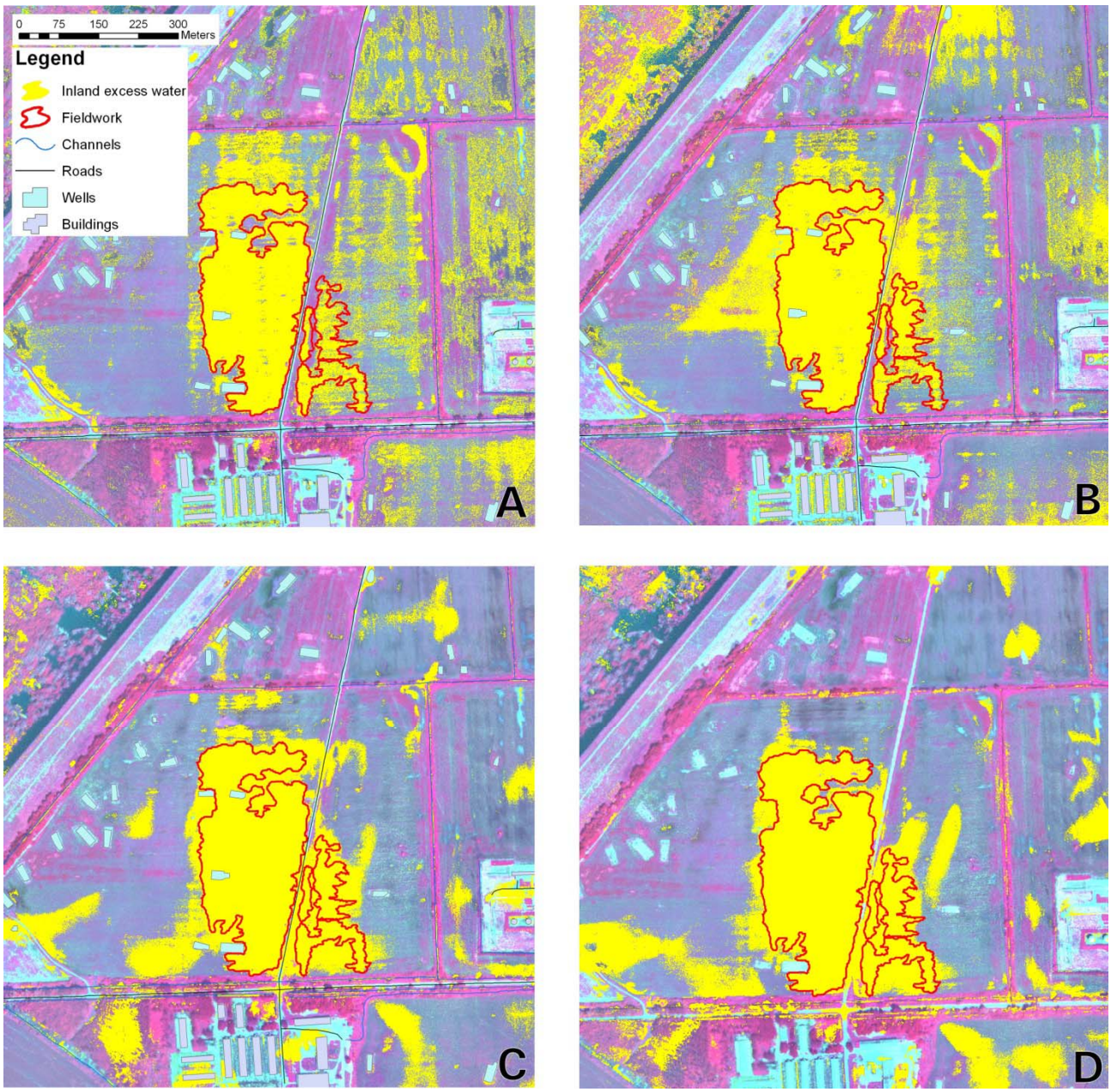

Figure 4. Evaluation of the input layers. All results cover the same area at the same scale.

Table 2 Input data for training and simulations on the training area.

	Description
1	Local depressions
2	Agrotopo soil characteristics
3	Distance from channels
4	Distance from roads
5	Distance from oil wells
6	Distance from buildings
7	Aerial photograph band 1
8	Aerial photograph band 2
9	Aerial photograph band 3

The first simulation is only based on the CIR images and the local depressions. The second also incorporated the distances to channels, the third simulation incorporates 8 input layers, only soil was excluded. The final simulation included all 9 input layers. The output maps of the four simulations are shown in figure 4.

The result of the simulation with only the color infrared images and the local depressions as input data shows a lot of the inland excess water pixels at the east part of the output map (A). It is unclear why in these places inundations show up. These areas are only partly characterized by local depressions. On the CIR images, they do not look much different from other areas either. During the fieldwork, they were not characterized as flooded areas. The overall accuracy of this classification is 88%.

Table 3. Spatial correlations between 9 input layers (1 – 9), the training layer and four simulation results (A - D).

	A	B	C	D	train	1	2	3	4	5	6	7	8	9
A	1.00	0.91	0.83	0.83	0.76[b]	-0.79	0.07	-0.30	0.14	0.13	0.06	0.23	0.02	0.04
B	0.91	1.00	0.91	0.91	0.83[c]	-0.73	0.06	-0.44	0.11	0.14	0.03	0.22	0.02	0.04
C	0.83	0.91	1.00	0.99	0.92[e]	-0.66	0.09	-0.40	0.18	0.17	0.11	0.19	0.02	0.03
D	0.83	0.91	0.99	1.00	0.92[f]	-0.66	0.09	-0.40	0.18	0.17	0.11	0.19	0.02	0.03
train	0.76	0.83	0.92	0.92	1.00	-0.59[a]	0.08	-0.37	0.16	0.16	0.09	0.18	0.02	0.03
1	-0.79	-0.73	-0.66	-0.66	-0.59	1.00	-0.05	0.19	-0.10	-0.06	-0.05	-0.12	-0.09	-0.12
2	0.07	0.06	0.09	0.09	0.08[g]	-0.05	1.00	0.28	0.46	0.33	0.34	0.03	-0.06	-0.06
3	-0.30	-0.44	-0.40	-0.40	-0.37[d]	0.19	0.28	1.00	0.27	0.07	0.31	-0.23	0.01	-0.02
4	0.14	0.11	0.18	0.18	0.16	-0.10	0.46	0.27	1.00	0.14	0.71	0.03	-0.07	-0.05
5	0.13	0.14	0.17	0.17	0.16	-0.06	0.33	0.07	0.14	1.00	-0.03	0.05	-0.01	-0.04
6	0.06	0.03	0.11	0.11	0.09	-0.05	0.34	0.31	0.71	-0.03	1.00	0.04	-0.11	-0.05
7	0.23	0.22	0.19	0.19	0.18	-0.12	0.03	-0.23	0.03	0.05	0.04	1.00	-0.13	0.26
8	0.02	0.02	0.02	0.02	0.02	-0.09	-0.06	0.01	-0.07	-0.01	-0.11	-0.13	1.00	0.63
9	0.04	0.04	0.03	0.03	0.03	-0.12	-0.06	-0.02	-0.05	-0.04	-0.05	0.26	0.63	1.00

The second simulation (B), with an overall accuracy of 91%, clearly shows a triangular shape from the central inland excess water area towards the west. This is an artificial area resulting from the *Distance to channels* map. The third simulation (C) incorporates all input layers except for the soil map. Its inland excess water pixels completely overlap with the fieldwork area, but identify also quite some inundations between the buildings in the southern part of the test area. This is a pig farm which was in use during the inland excess water period and was not suffering from any flooding. This training result had an overall accuracy of 93% and was used for the simulation shown in figure 3. The fourth simulation (D) incorporates all input layers. Its overall accuracy is 91% which is slightly lower than the result without the soil layer. The result looks very similar to the third simulation and the additional effect of the soil layer is not clear. This should be contributed to the lack of variation in infiltration characteristics between the three soil classes in the area.

The spatial correlations between the different input layers and output results show which layers play an important role in the simulation and which layers are less important (Table 3). The first simulation result clearly shows the depressions in the area (Fig. 4 A). These depressions have a correlation of -0.59 with the fieldwork data (Table 3. a). This correlation is negative because the depression classes range from no depression to deep depression and the inland excess water ranges from inland excess water to no inland excess water. The relatively high value shows that the relief has a strong influence on the formation of inland excess water. The spatial correlation between the simulation and the fieldwork data is 0.76 (Table 3.b). If the layer with distances from channels is added to the simulation the correlation increases to 0.83 (Table 3.c). There exists a correlation between the individual channel distance layer and the fieldwork data although it is not very high: 0.37 (Table 3.d). If 8 layers are used in the simulation, the correlation further increases to 0.92 (Table 3.e), although the correlation between the individual layers (distances maps, and CIR bands) and the fieldwork data is low. Adding the soil input layers to the simulation does not result in a higher correlation (Table 3.f). The limited influence of the soil in the simulations in this study area is also reflected in the low spatial correlation (0.08) between the fieldwork data and the soil map (Table 3.g).

5. CONCLUSIONS

The artificial neural network – Geographic information system framework is capable of identifying inland excess water. It also allows for the flexible adaptation of the network parameters, which makes it an efficient environment to test different settings for the neural networks. Optimization parameters have been incorporated to improve its computational efficiency and to prevent the calculations to run out of memory. It was found that in this study area relief has a very important influence, while the influence of the soil is small, because of its the limited variation. If *distance to anthropogenic* objects is included in the training and simulation, the results improve. The distance to channels is the most influential anthropogenic factor. Overall, a very high correlation exists between the simulation output results and the fieldwork data.

Future research aims to extend the study area to other parts of the Carpathian basin, where different types of inland excess water occur and where different factors influence its formation.

ACKNOWLEDGEMENT

This study was financially supported by the project "Development of an INLAND EXCESS WATER-INFO system" (Economic Operative Program: GOP - 1.1.1 - 08 / 1 -2008 – 0025).

REFERENCES

Agrotopo, 2002**,** *Hungarian Agrotopographic database*, Magyar Tudományos Akadémia Talajtani és Agrokémiai Kutatóintézet, Budapest. (in Hungarian).

Atkinson, P.M. & Tatnall, A.R.L., 1997, *Introduction neural networks in remote sensing*. International Journal of Remote Sensing, 18, 699-709.

Bishop, C.M., 1995, *Neural networks for pattern recognition.* Oxford university press, 482.

Bozán, Cs, Körösparti, J., Pásztor, L., Kuti, L., Kozák, P. & Pálfai, I., 2009, *GIS-based Mapping of excess water inundation hazard in Csongrád county (Hungary).* Proceedings of the International Symposia on Risk Factors for Environment and Food Safety & Natural Resources and Sustainable Development, Oradea 2009, 678-684.

Demuth, H., Beale, M. & Hagan, M., 2010. *Neural Network Toolbox 6, User's Guide*. The Mathworks, 901.

Hagen, M.T., Demuth H.B. & Beale, M.H., 1996, *Neural Network Design.* Boston, MA., PWS Publishing, 734.

Hewitson, B.C. & Crane, R.G., 1994. *Neural Nets: Applications in Geography*. Dordrecht: Kluwer Academic Publishers, 194.

Ianos, I, Peptenatu D. & Zamfir D., 2009, *Respect for environment and sustainable development*. Carpathian Journal of Earth and Environmental Sciences, 4,1, 81-93.

van Leeuwen B., Szatmári J., Tobak Z., Németh Cs. & Hauberger G., 2009a, *Opportunities for the generation of high resolution digital elevation models based on small format aerial photography.* HunDEM Conference Proceedings, 2009, Miskolc, Hungary, 5.

van Leeuwen B., Tobak Z., Szatmári J., Mucsi L., Kitka G., Fiala K., Rakonczai J. & G. Mezősi, 2009b, *Small format aerial photography: a cost effective approach for visible, near infrared and thermal digital imaging*. In: A. Car, G. Griesebner, J. Strobl (eds.), Geospatial Crossroads @ GI_Forum' 09, Proceedings of the Geoinformatics Forum Salzburg, Heidelberg, 2009, 200-209.

van Leeuwen B., Tobak Z., Szatmári J. & Barta K., 2010, *Application of new methods in the analysis of the formation and monitoring of inland excess wate).* In: Lóki J., Demeter G. (eds.) Az elmélet és gyakorlat találkozása a térinformatikában I, Debrecen, 121-130. (in Hungarian)

Kuti L., Kerék B. & Vatai J., 2006, *Problem and prognosis of excess water inundation based on agrogeological factors.* Carpathian Journal of Earth and Environmental Sciences, 1, 1, 5-18.

Mezősi G., 2011, *Environmental capabilities, hazards and conflicts.* Univ Kiadó, Szeged, 214.

Pálfai, I., 2003, *Inland excess water vulnerability map of Hungary*. Vízügyi közlemények, 83, 3, 376–392 (in Hungarian)

Pálfai, I., 2004, *Inland excess water and droughts in Hungary*. Hidrológiai tanulmányok, Budapest, 492. (in Hungarian)

Pásztor, L., Pálfai, I., Bozán, Cs., Kőrösparti, J., Szabó, J., Bakacsi, Zs. & Kuti, L., 2006. *Spatial stochastic modelling of inland inundation hazard*. 9th AGILE Conference on Geographic Information Science. Visegrád, Hungary 2006, 139-143.

Pradhan, B. & Lee, S., 2010. *Landslide susceptibility assessment and factor effect analysis: backpropagation artificial neural networks and their comparison with frequency ratio and bivariate logistic regression modelling*. Environmental, Modelling & Software, 25, 747-759.

Rakonczai J. , Csató Sz., Mucsi L., Kovács F. & Szatmári J., 2003. *Practical experiences with identification of inland excess water in the year 1999 and 2000.* Vízügyi Közlemények 1998-2001. évi árvízi külön füzetek, 4, 317-336. (in Hungarian)

Rakonczai, J, Farsang, A., Mezősi, G. & Gál, N., 2011, *Theoretical background of inland excess water formation.* Földrajzi Közlemények, 135, 4, 339-350. (in Hungarian)

Szatmári, J.; Szijj, N.; Mucsi, L.; Tobak, Z.; van Leeuwen, B.; Lévai, Cs. & Dolleschall, J., 2011. Mapping of inland excess water and spatial data acquisition for modeling of the formation of inland excess water. In. Lóki J. (szerk.) Az elmélet és gyakorlat találkozása a térinformatikában II., Debrecen, 27-35. (in Hungarian)

Tobak Z., Szatmári J. & van Leeuwen B., 2008**,** *Small format aerial photography – remote sensing data acquisition for environmental analysis*. Journal of Env. Geogr I, 3-4, 21-26.

Vízügy 2011, 2011, *Information about the Inland excess water situation 2010-2011*, Budapest (In Hungarian)

Yang, Y. & Rosenbaum, M.S., 2001, *Artificial networks linked to GIS for determining sedimentology in harbours*. Journal of Petroleum Science and Engineering, 29, 213-220.

Zhou, W, 1999, *Verification of the nonparametric characteristics of backpropagation neural networks for image classification*. IEEE Transactions on geoscience and remote sensing, 37, 2, 771-779.

Receievd at: 05. 03. 2012
Revised at: 06. 09. 2012
Accepted for publication at: 22. 09. 2012
Published online at: 24. 09. 2012